

2356-10

Targeted Training Activity: ENSO-Monsoon in the Current and Future Climate

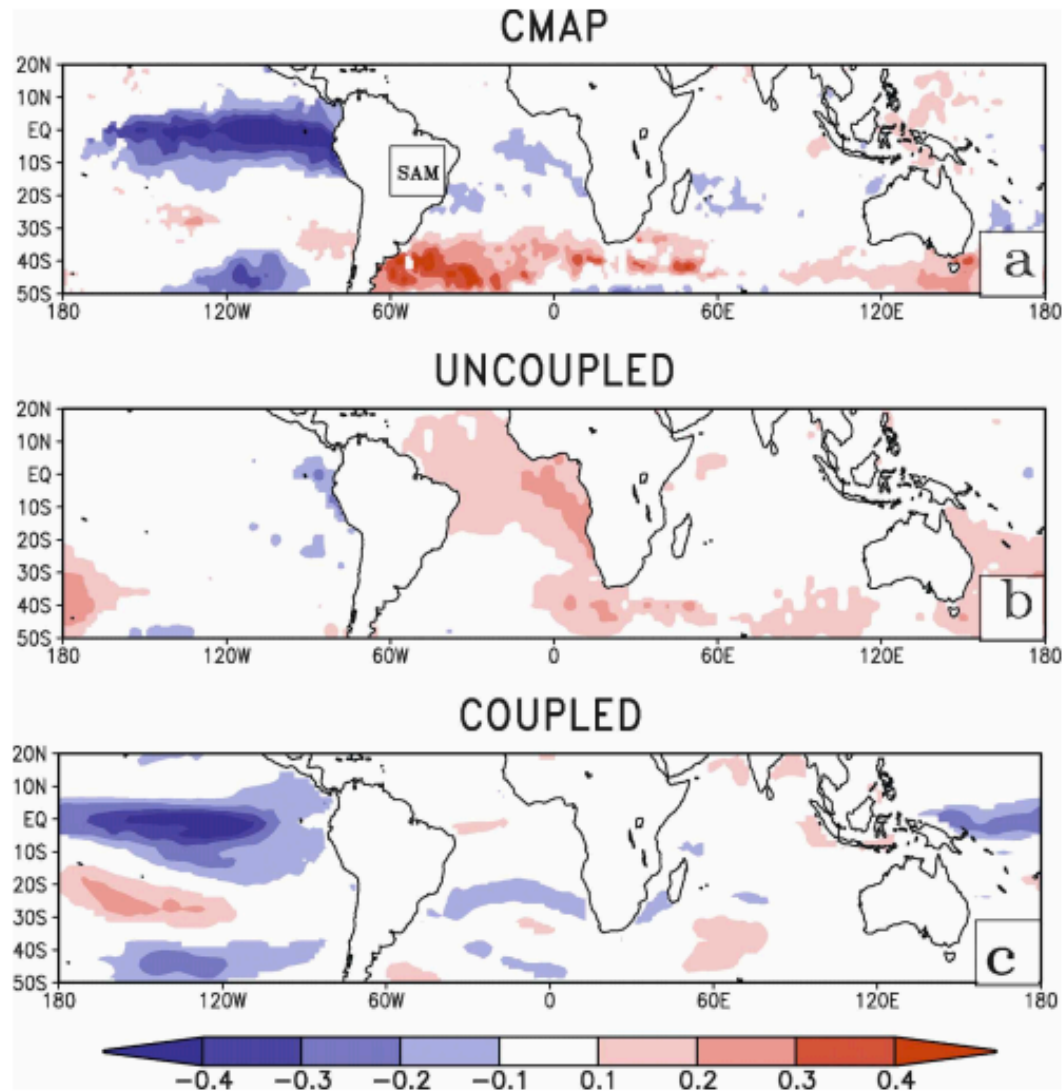
30 July - 10 August, 2012

ENSO American Monsoons Teleconnections

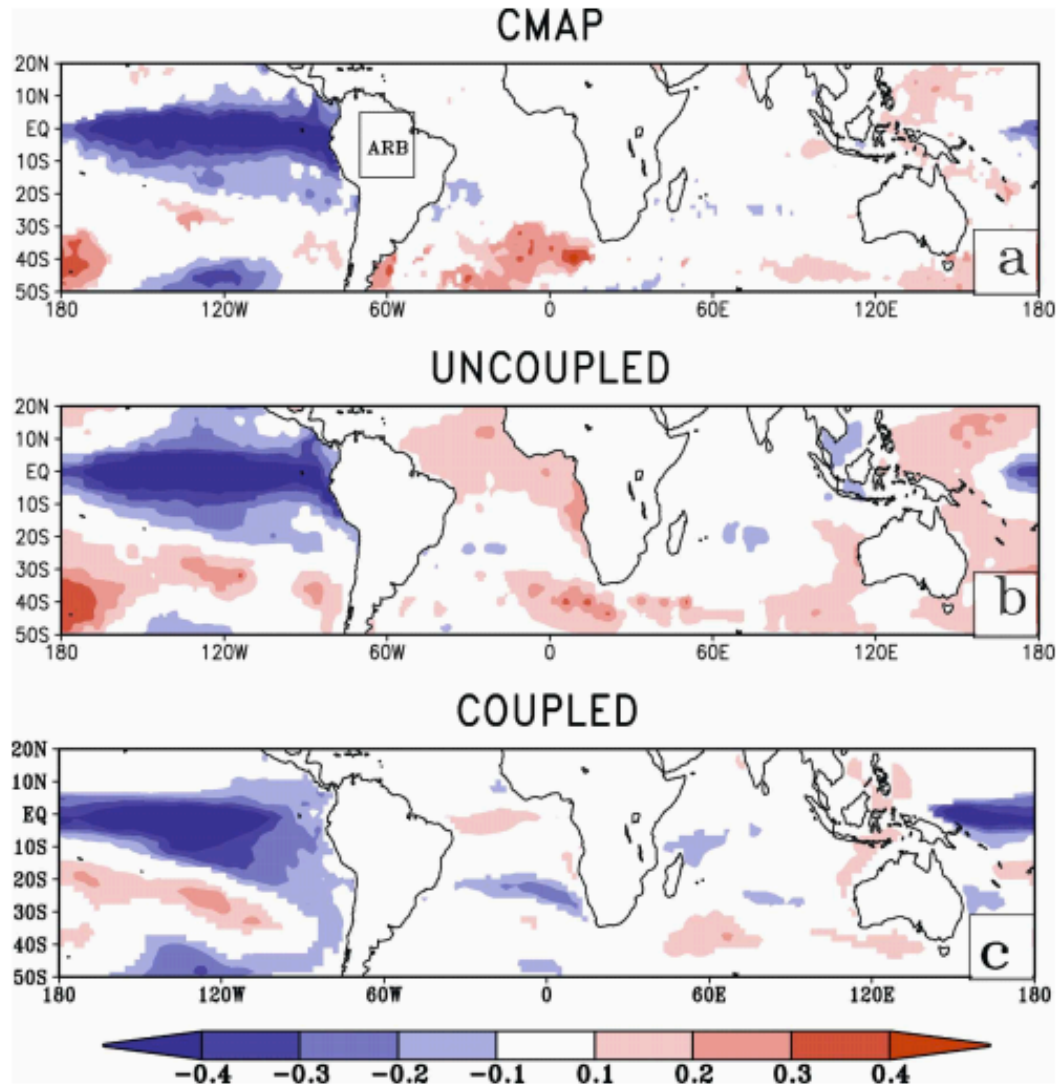
MISRA Vasubandhu
*Florida State University
Department of Earth, Ocean and Atmospheric Sciences
404 Love Building, 1017 Academic Way
Tallahassee FL 32306
U.S.A.*

American Monsoons-ENSO teleconnection

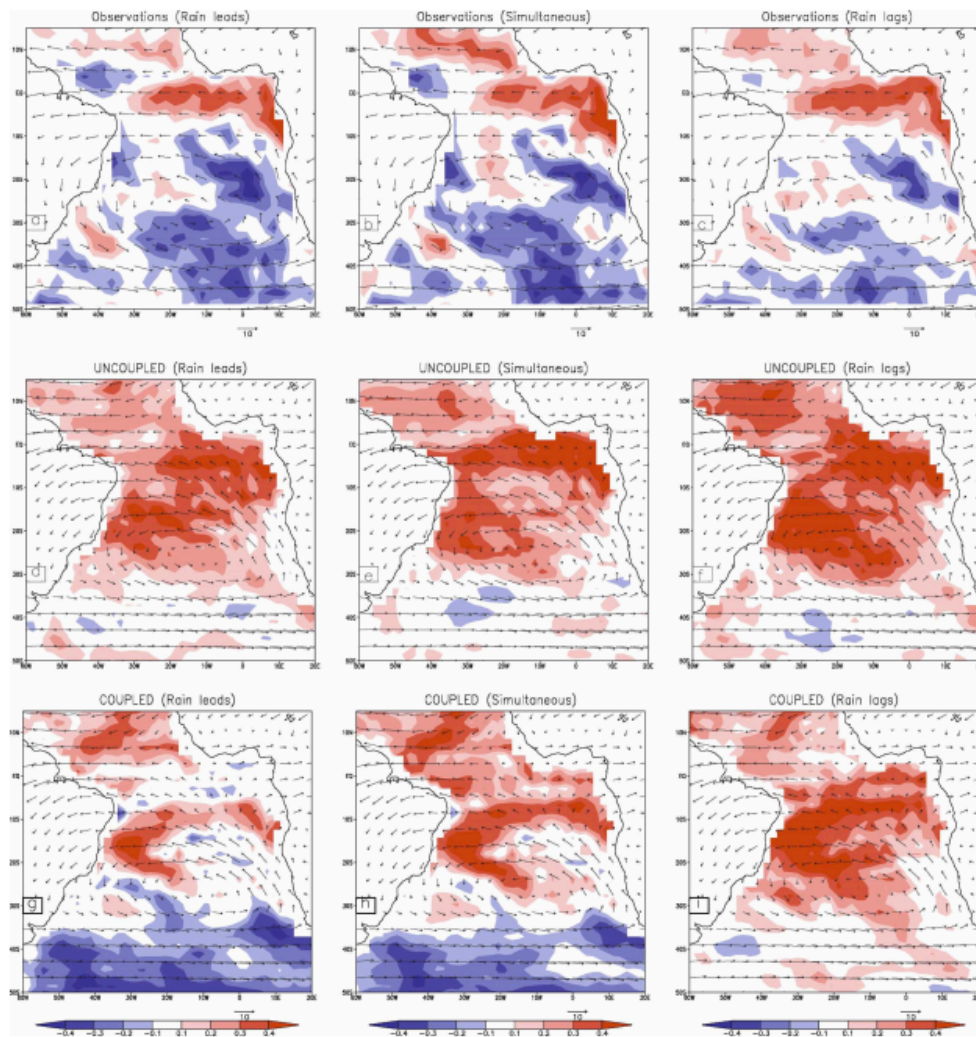
Vasu Misra,
Dept. of Earth, Ocean and Atmospheric Science,
Florida State University
Email: vmisra@fsu.edu



Linear regression of mean DJF rainfall over the SAM (boxed) region on tropical SST from a) observations, and the last 50 years of a 100 year integration of a b) uncoupled AGCM and c) coupled to ocean AGCM. The AGCM's in b and c are identical.



Linear regression of mean DJF rainfall over the ARB (boxed) region on tropical SST from a) observations, and the last 50 years of a 100 year integration of a b) uncoupled AGCM and c) coupled to ocean AGCM. The AGCM's in b and c are identical.



Correlation of rain with SST. Negative correlations in the left column suggest atmospheric forcing of SST

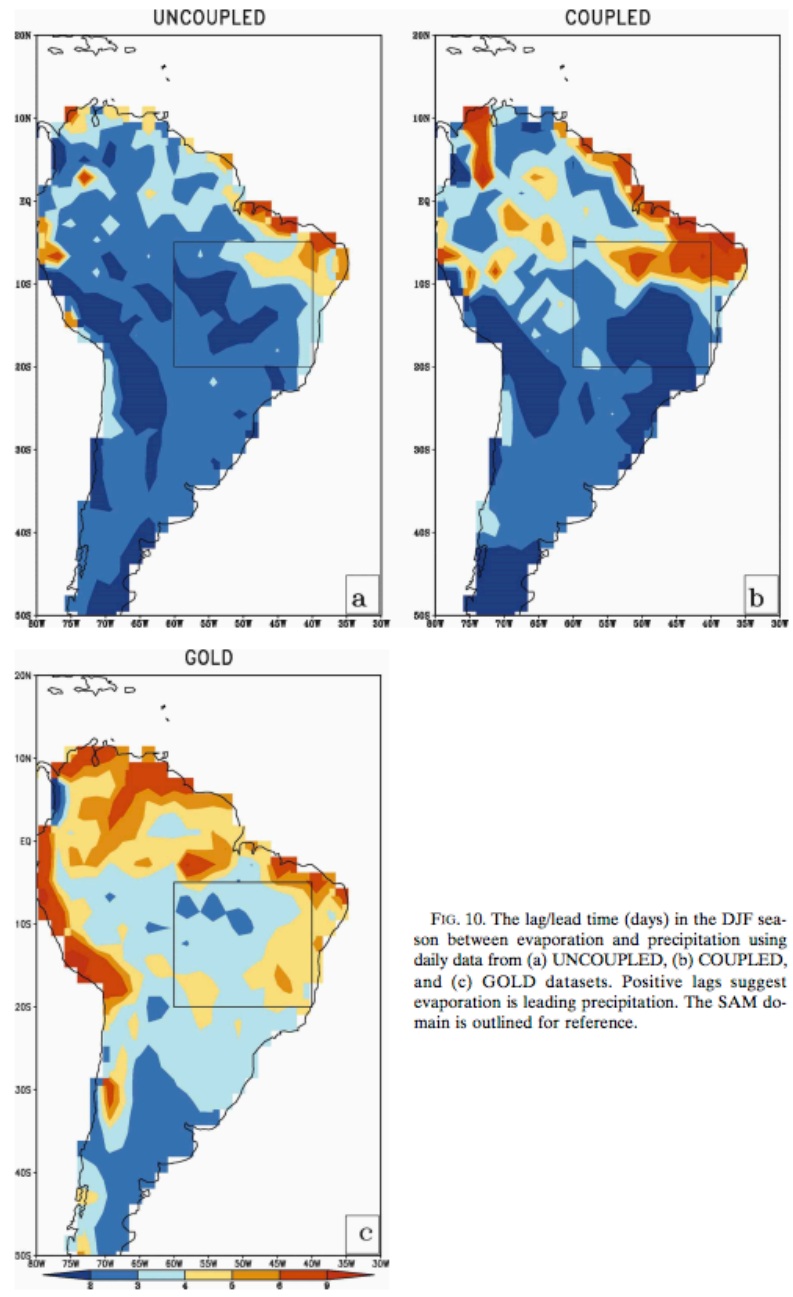
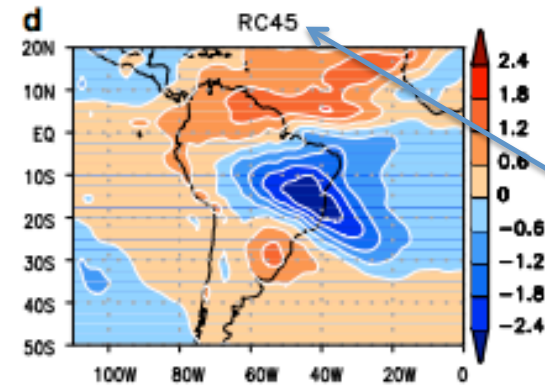
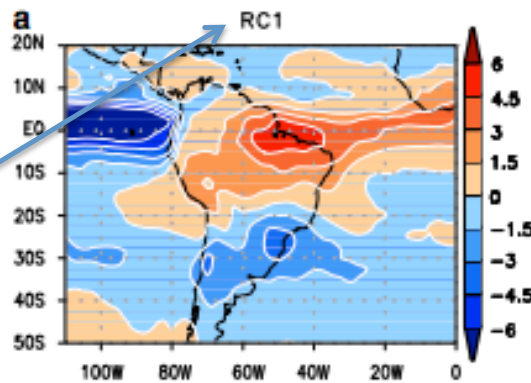


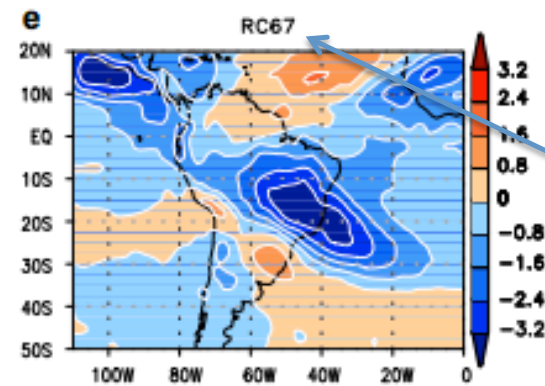
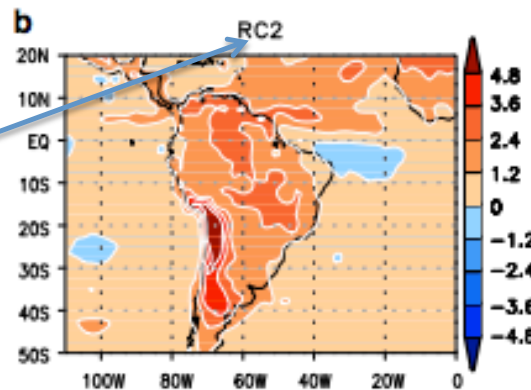
FIG. 10. The lag/lead time (days) in the DJF season between evaporation and precipitation using daily data from (a) UNCOUPLED, (b) COUPLED, and (c) GOLD datasets. Positive lags suggest evaporation is leading precipitation. The SAM domain is outlined for reference.

Related to ENSO



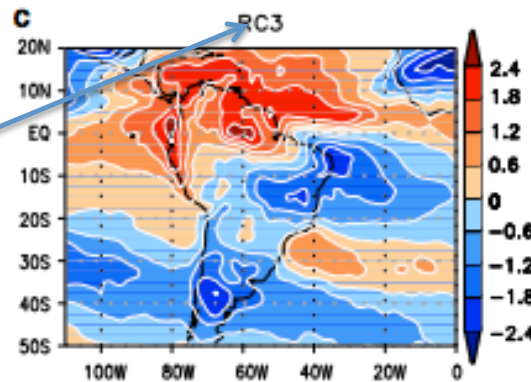
Inter-seasonal mode (165 days; NAO)

Related to AMO

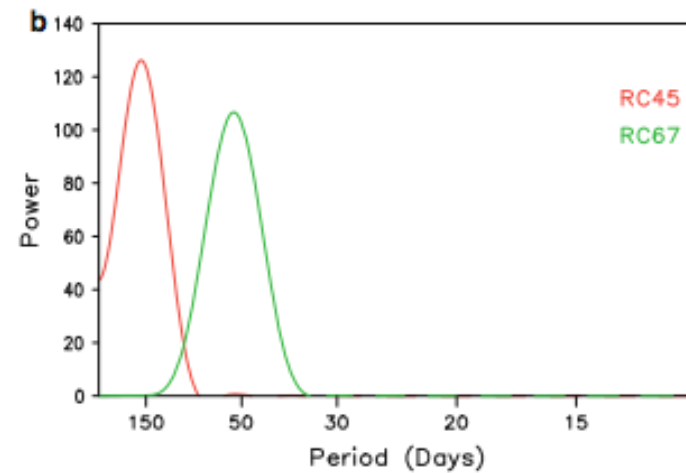
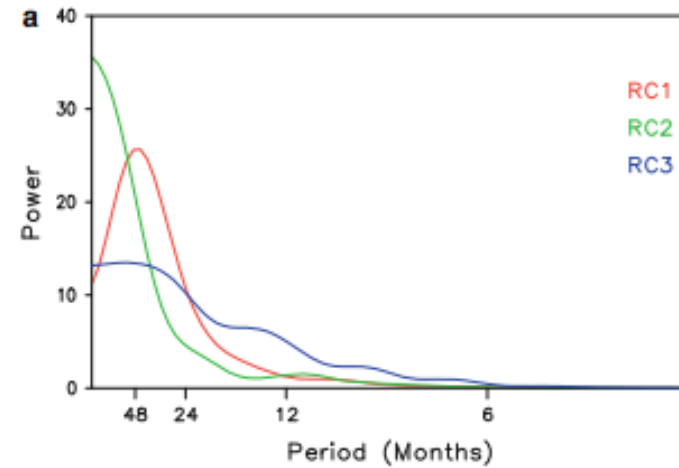
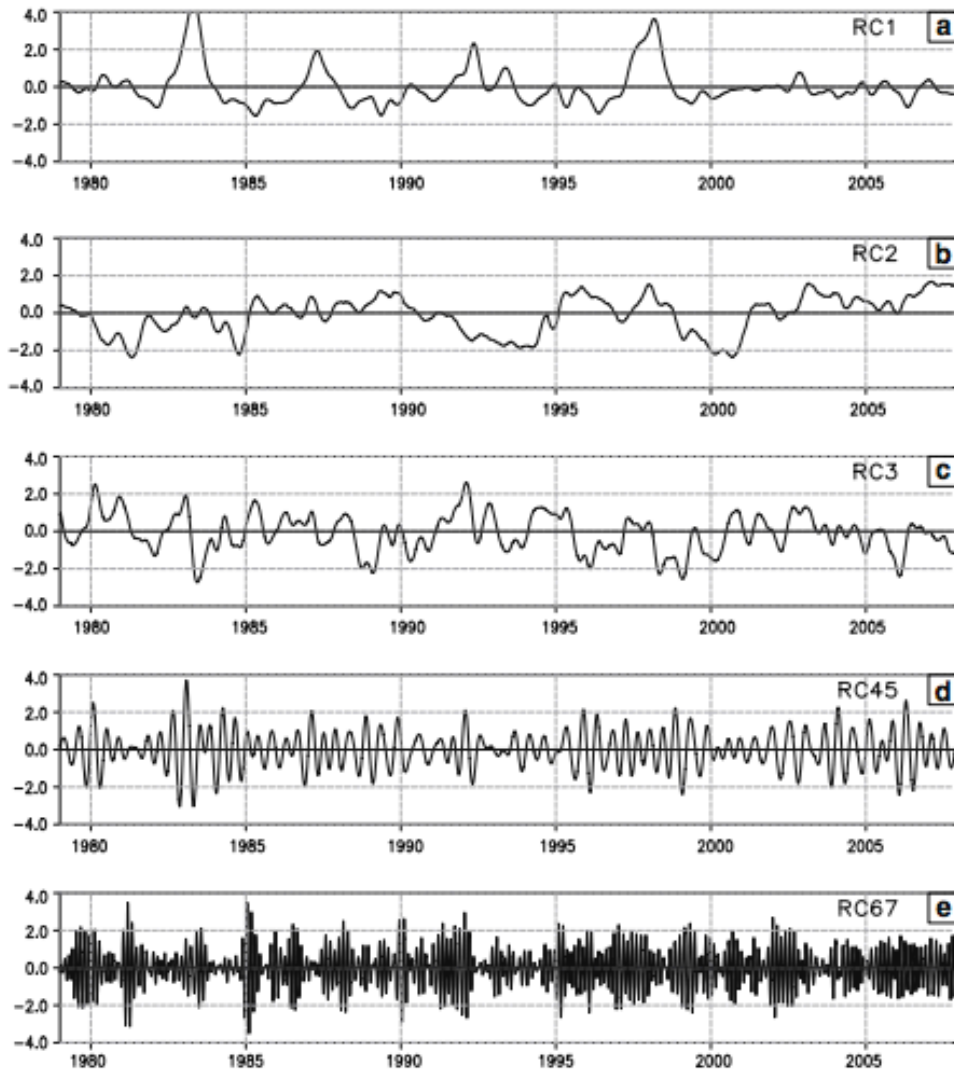


52 day-MJO

Related to PDO

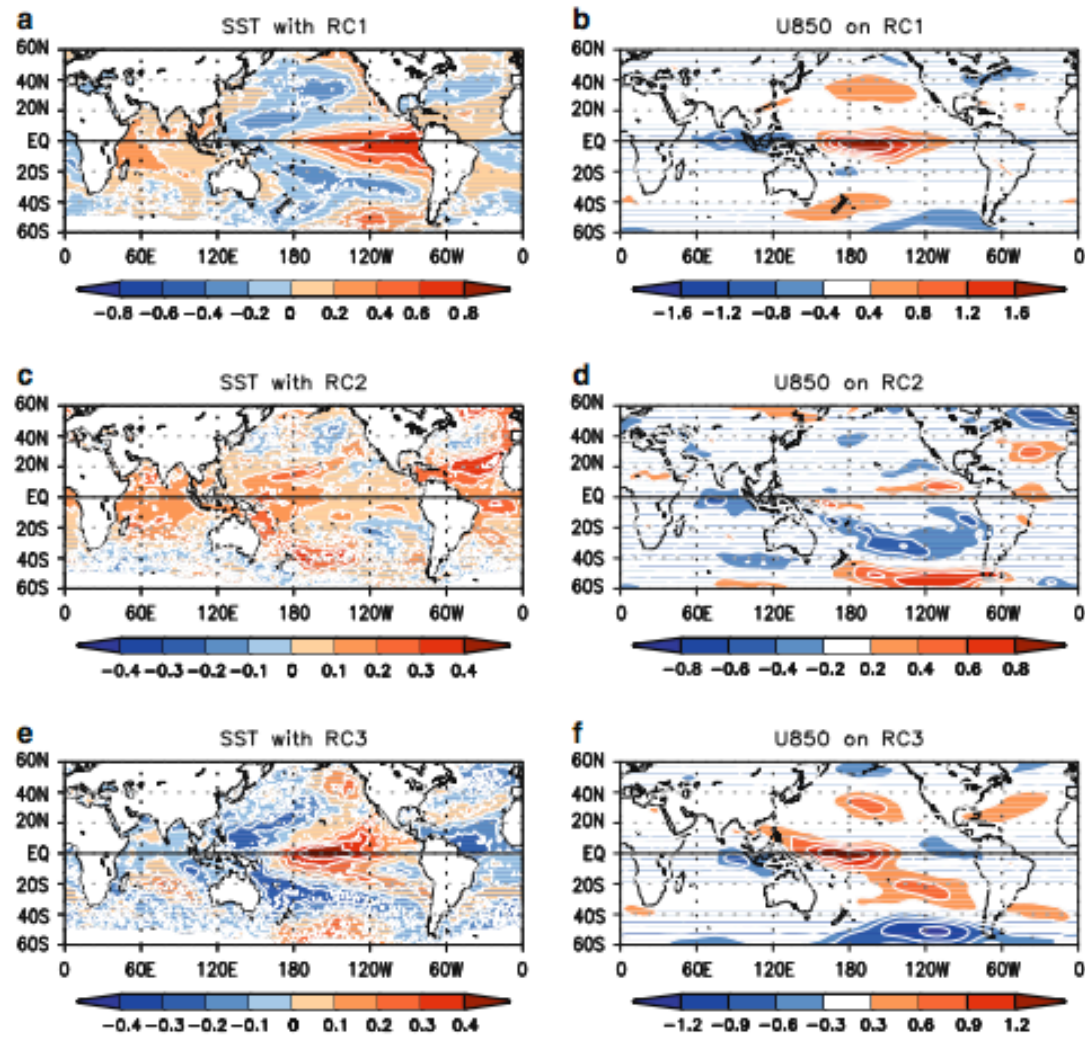


Spatial patterns of the dominant first 7 modes of variations of OLR over the domain

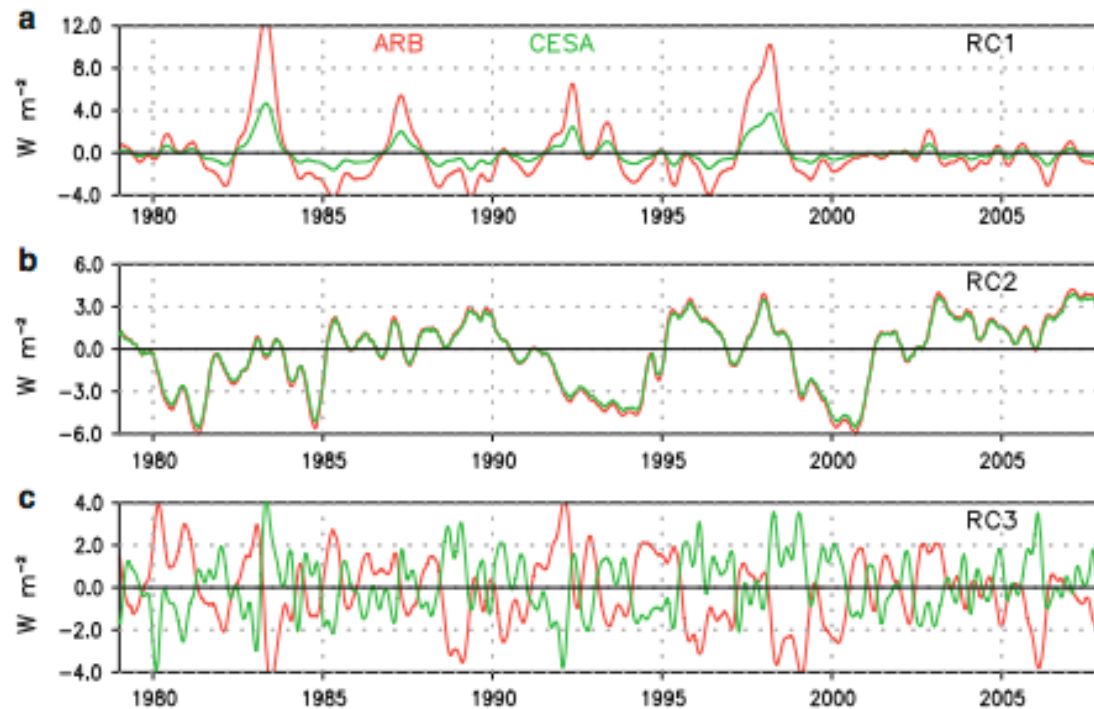


Temporal variability of the EOF's from previous slide of the first 7 modes of variations of OLR over the domain

Power spectrum of the PC's on the left



Correlations of PC's of OLR on global SST (left) and zonal wind (right)



Time series of the reconstructed OLR from a) EOF1 (ENSO), b) EOF2 (AMO), c) EOF3 (PDO) components over the ARB (red) and SAM (green) domains. Note that the PDO signal in ARB and SAM are conflicting, which makes interannual variations of the two region different. From Krishnamurthy and Misra (2010).

$$A(\text{day}) = \sum_{n=1}^{\text{day}} (R(n) - \bar{R})$$

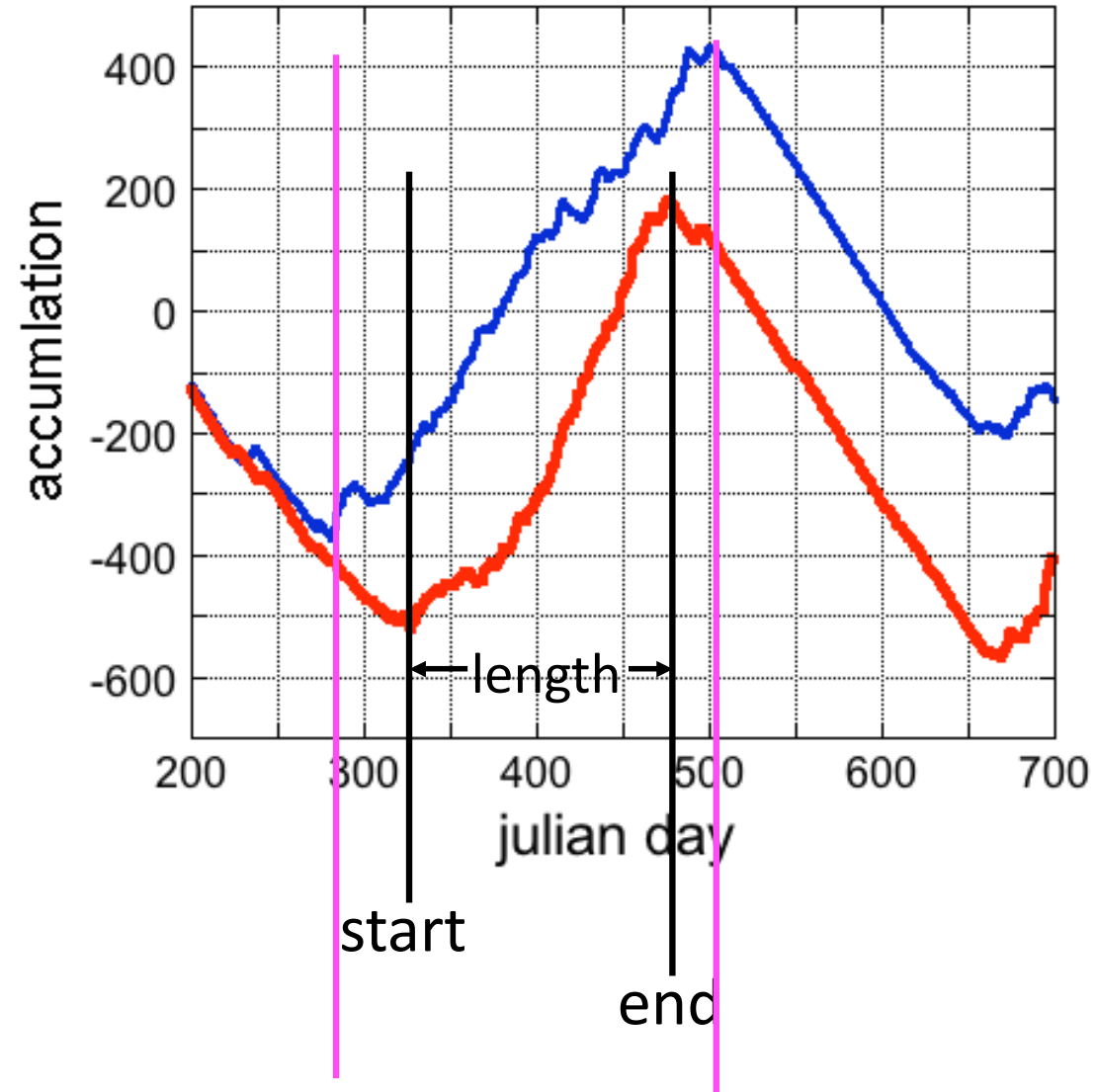
$A(\text{day})$ = Anomalous accumulation

$R(n)$ = daily rainfall

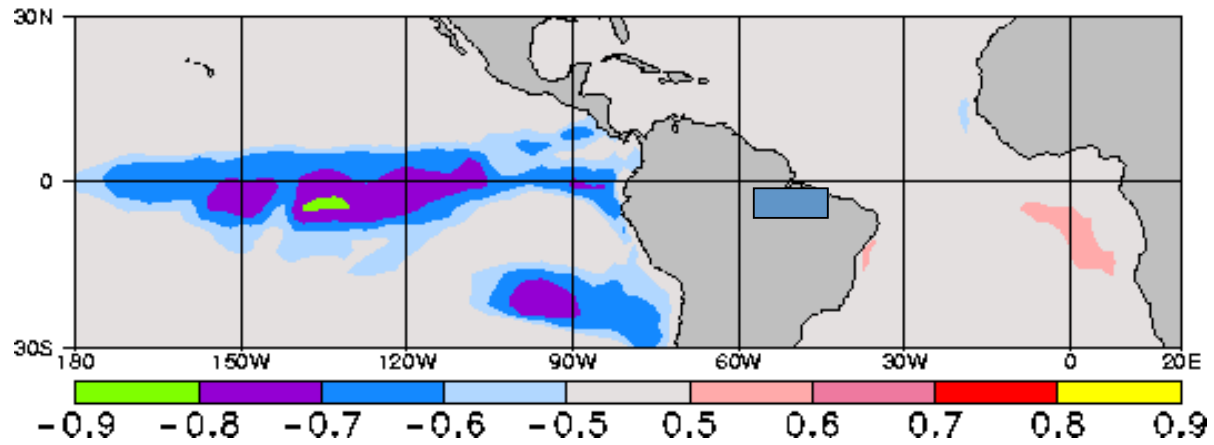
\bar{R} = annual average daily precipitation

The rainy season is considered to be when the slope of the curve is positive ($R(n) > \bar{R}$).

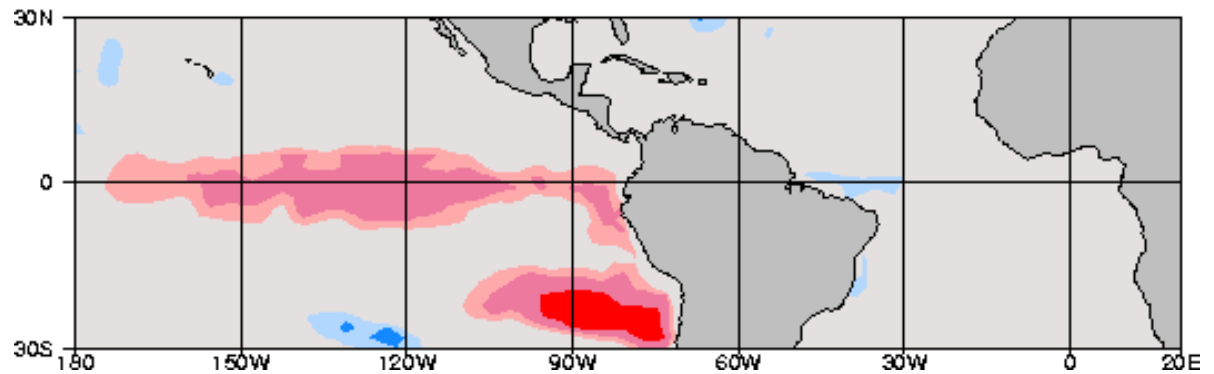
Anomalous Accumulation 53.4W, 7.0S (central Amazon)



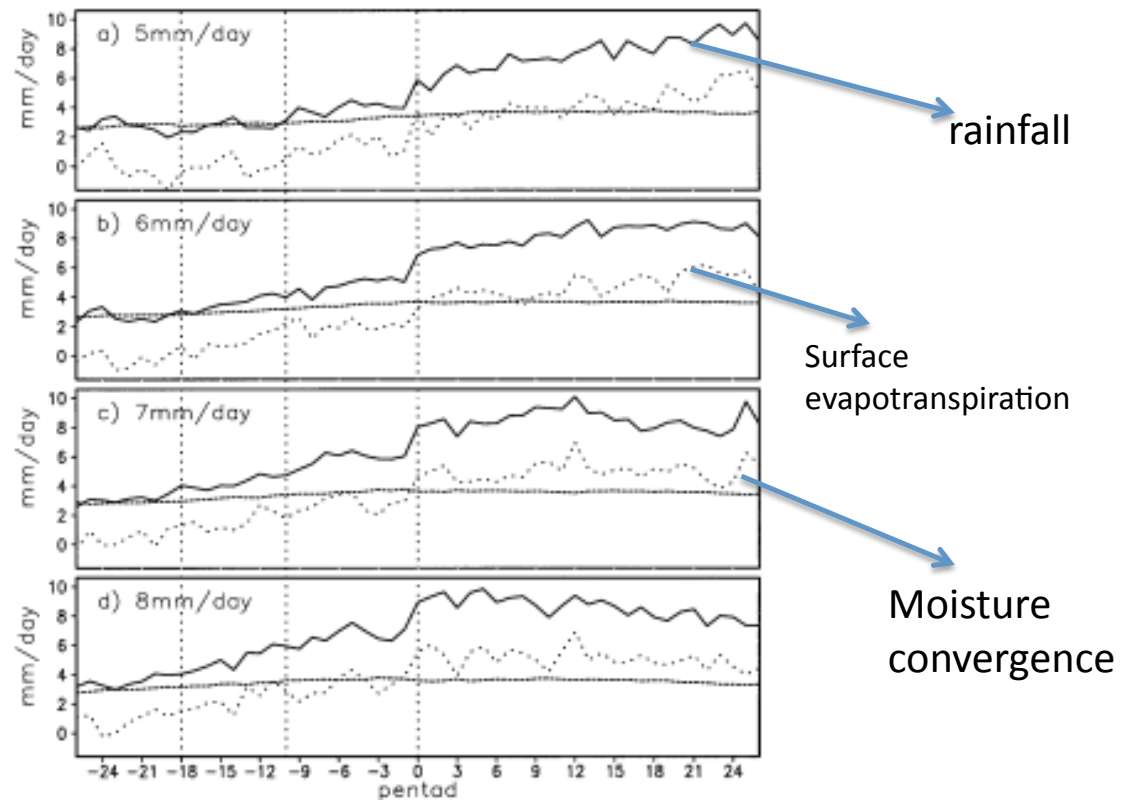
DJF total rainfall versus SST



Start versus SST



Most of the interannual variations in rainfall over equatorial Amazon due to ENSO is recovered from the onset date



Onset is defined as the time after which rainfall exceeds a certain value for six out of eight subsequent pentads and is well below the threshold in six out of the eight preceding pentads.

Behavior of the surface meteorology around the onset date (defined at various thresholds) over the ARB region. 0 pentad is the onset. Surface evaporation more than moisture flux convergence is increasing the precipitation---role of biosphere is quite important.

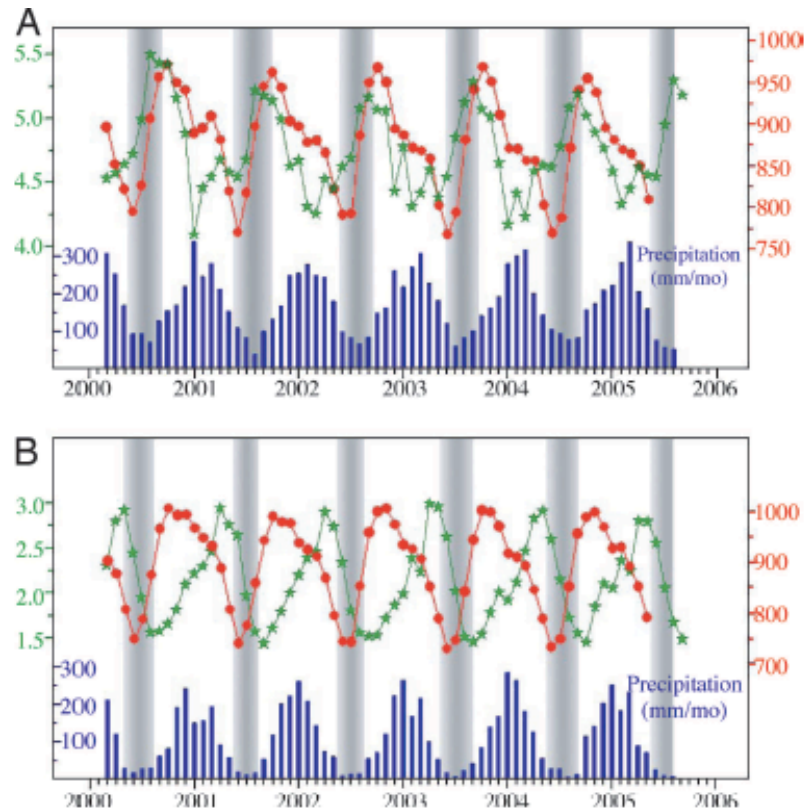
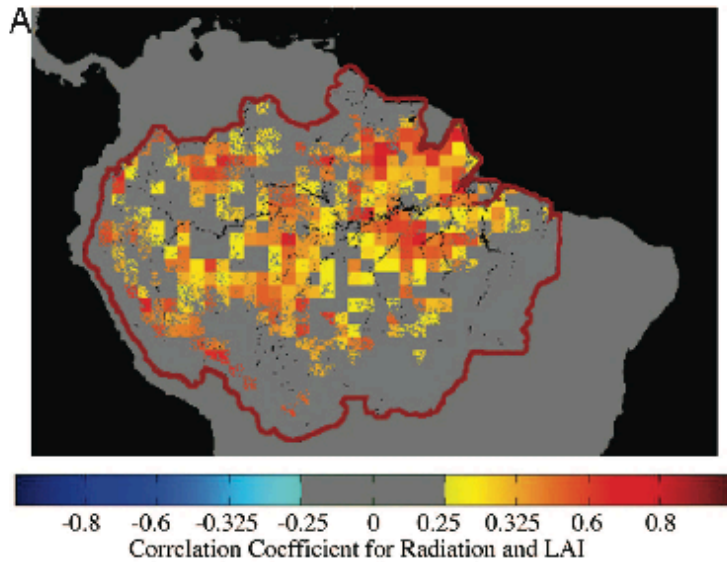


Fig. 1. Time series of monthly LAI from the Terra MODIS instrument (green), monthly maximum of hourly average surface solar radiation from the Terra Clouds and the Earth's Radiant Energy System (CERES) and Geostationary Operational Environmental Satellite 8 (GOES-8) instruments (red), and monthly merged precipitation from the Tropical Rainfall Measuring Mission (TRMM) and other sources (blue). (A) Time series based on data averaged over all Amazon rainforest pixels, as identified in the MODIS land cover map (SI Fig. 4B), south of the equator. The start of the data record is March 2000 and the end points are September 2005 (LAI), May 2005 (solar radiation), and August 2005 (precipitation). The shaded areas denote dry seasons, defined as months with precipitation < 100 mm or less than one-third the precipitation range $[0.33(\text{maximum} - \text{minimum}) + \text{minimum}]$. The solar radiation data are for all sky conditions and include direct and diffuse components. (B) Same as A except that the data are from savanna and grassland pixels adjacent to the Amazon basin in Brazil and south of the equator (SI Fig. 4B). The shaded areas denote dry seasons, defined as months with precipitation < 50 mm. Information on the data is given in SI Materials and Methods.

The aggregate phenological cycle of leaf flushing and abscission leads the seasonal cycle of the solar radiation, with higher LAI in drier seasons when solar radiation is high than in wet season. In an evergreen forest, older leaves that are photosynthetically less efficient with poor stomatal control are exchanged for numerous new leaves.

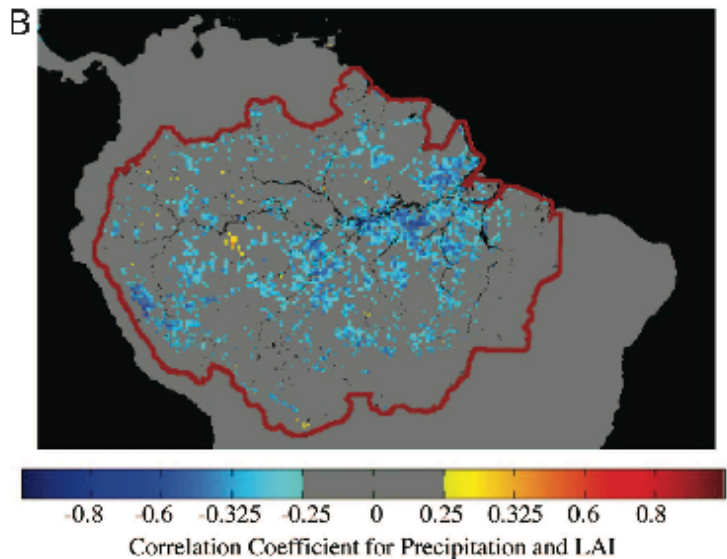
The surrounding savannah behaves in just the opposite way (more LAI in wet season) to deep rooted, generally well hydrated but light limited Amazon rain forest

Large seasonal swings in leaf area of Amazon rainforests



Changes in LAI are both positively correlated with changes in solar radiation and negatively correlated with changes in precipitation. But the correlations between LAI and radiation are larger and at the pixel level more numerous.

The negative correlations between LAI and precipitation are likely an indirect effect of the changes in cloudiness and radiation associated with precipitation changes.

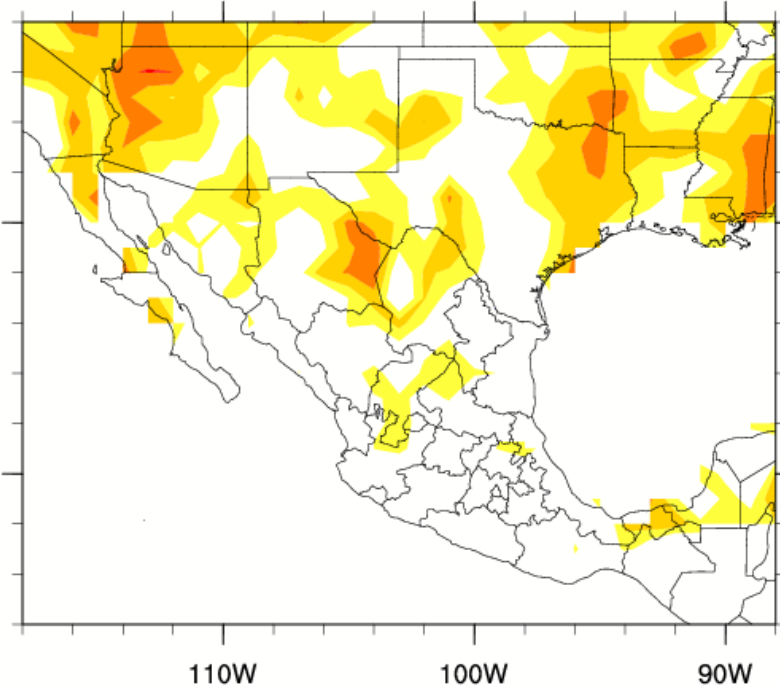


An increase in the surface evapotranspiration at the end of the dry season appears to be the primary cause of increased buoyancy of surface air, which consequently increases the probability of atmospheric convection.

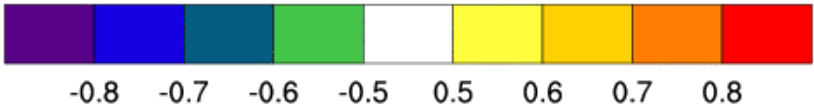
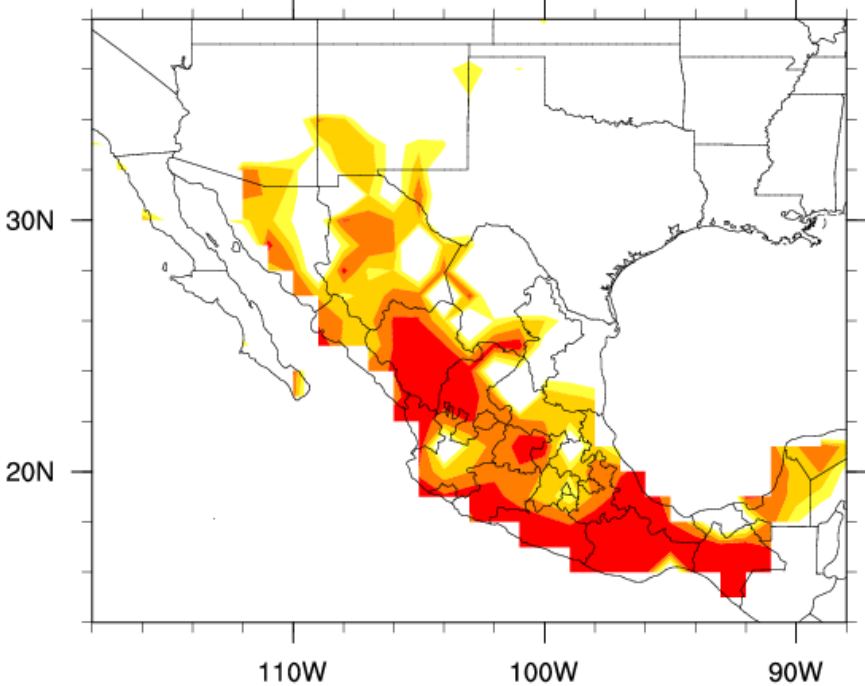
A 25% increase in LAI over 60% of Amazon forest during the dry season therefore suggests a potentially important role of vegetation in controlling the initiation of the wet season. 15

May - September Total Precipitation

Versus Wet Season Length

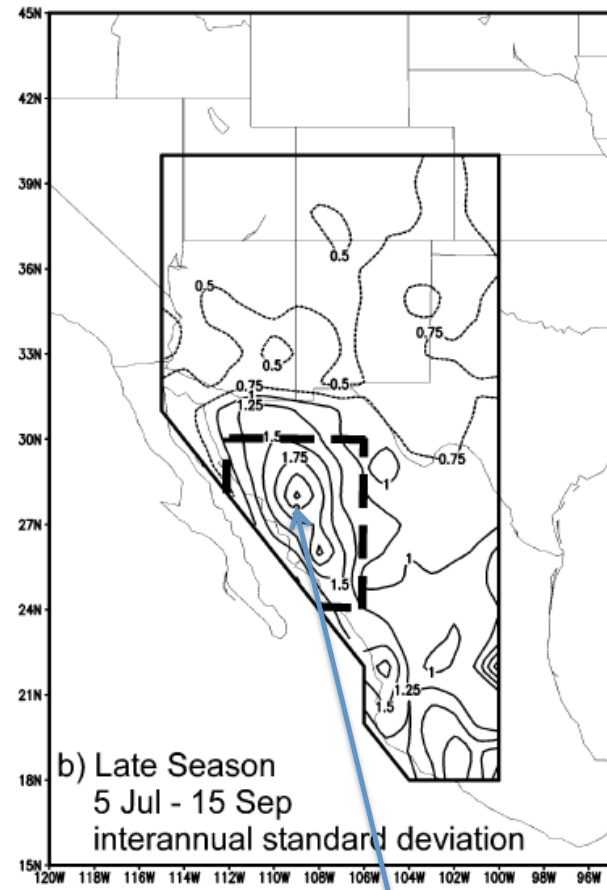
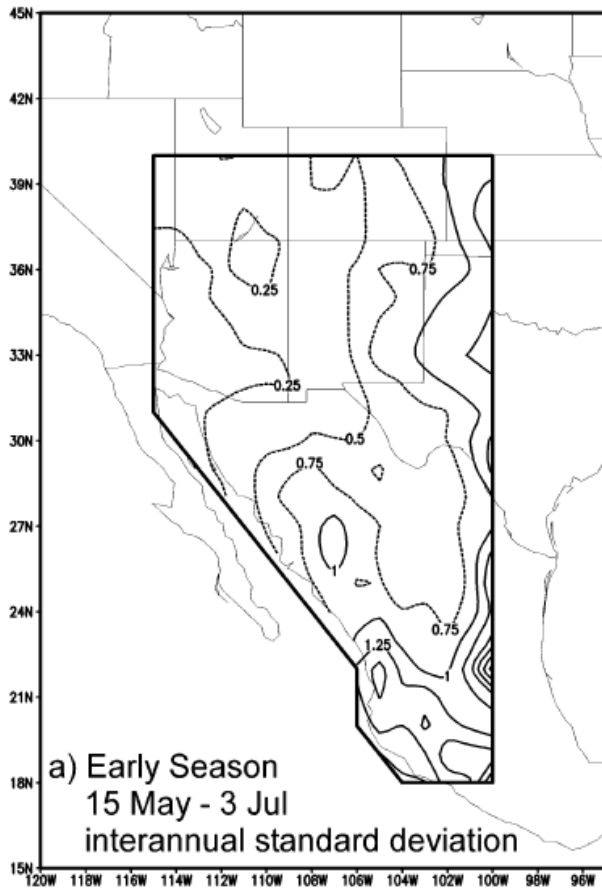


Versus Wet Season Rate



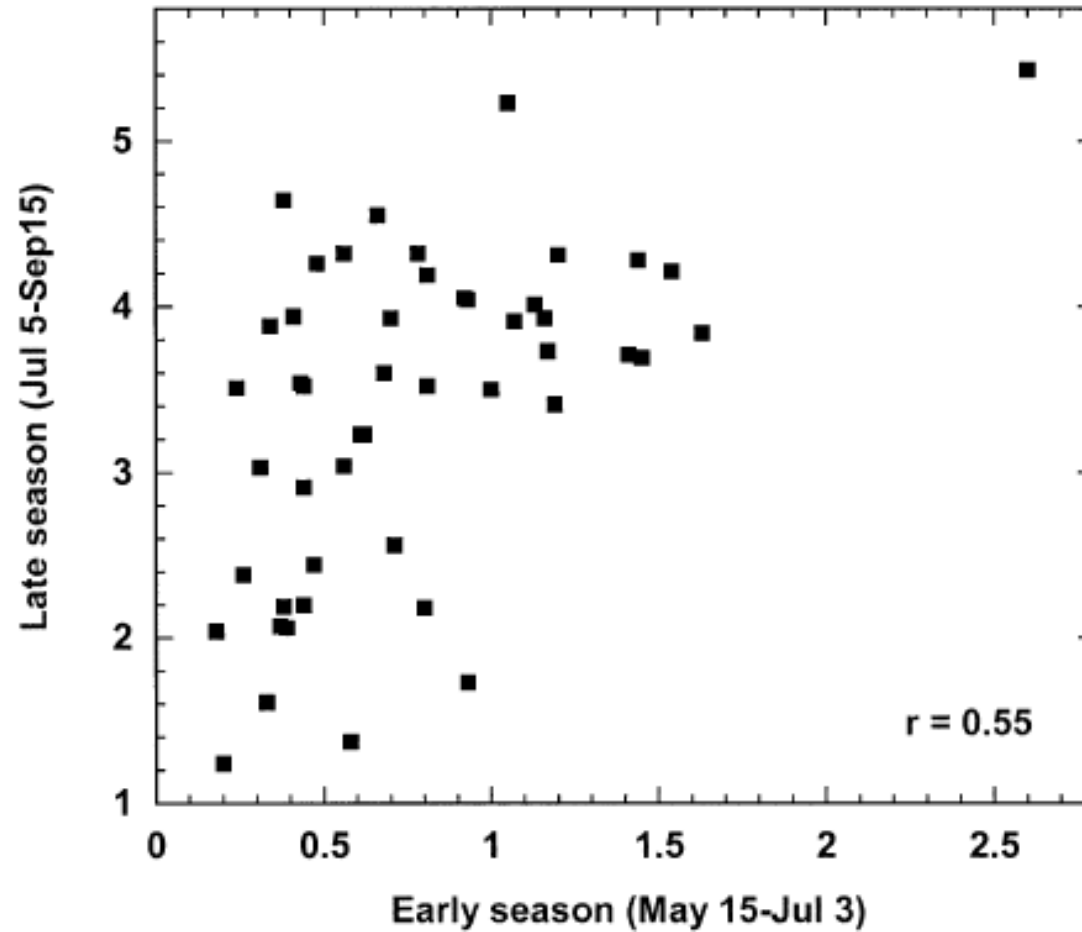
correlation

Standard deviation of monsoon rainfall



Core of the NAM

In the core region of NAM



The non-linear relationship of early to late season NAM rainfall supports the concept that an anomalously wet land surface across the core precipitation region in the early season helps promote the continuation of anomalously wet conditions in the late season. However, no such persistence of dry conditions is apparent in the data.

Correlation of NAM rainfall with ENSO is poor

Precipitation index	Mean (mm day ⁻¹)	Correlation coefficients		
		Core/late	Niño-3.4/ JF	Niño-3.4/ MJ
Core early season	0.79	0.55	-0.29	-0.14
Core late season	3.40	1.00	-0.12	-0.09

Some studies suggest some very limited predictability of NAM summer precipitation in New Mexico and Arizona associated with snow water equivalent or proxies for this variable. However, these studies relate only to the relatively modest monsoon precipitation on the very northern boundaries on the overall NAMS precipitation regime.

Precipitation index	Mean (mm day ⁻¹)	Correlation coefficients		
		Core/late	Niño-3.4/JF	Niño-3.4/MJ
(a) 1951–76, pre-PDO shift				
Core early season	0.74	0.48	−0.19	0.08
Core late season	3.19	1.00	−0.16	−0.10
(b) 1977–98, post-PDO shift (1979–98 for YW index correlations)				
Core early season	0.86	0.67	−0.46	−0.39
Core late season	3.70	1.00	−0.21	−0.27

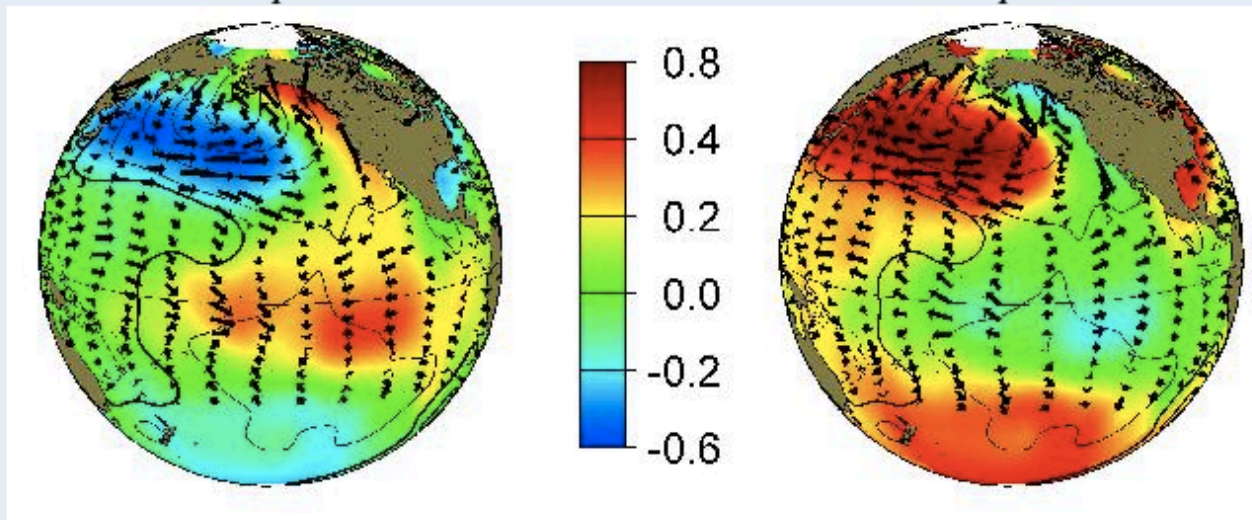
The Table above suggests that negative correlations between Niño-3.4 and early-season core precipitation are enhanced during PDO-positive decades, such as occurred after 1976.

The positive correlation between early and late seasons (i.e., anomaly persistence) is particularly pronounced after the PDO shift in 1976.

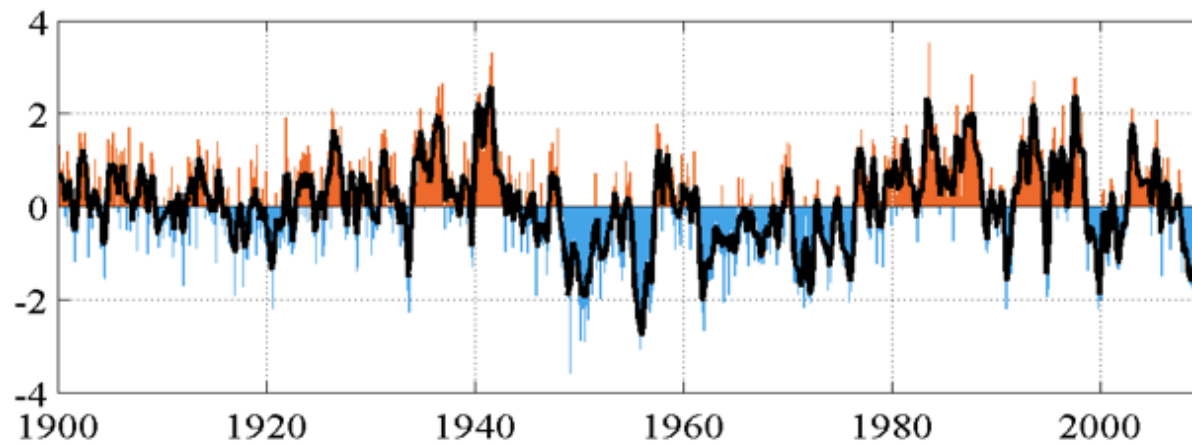
warm and cool phases of PDO

warm phase

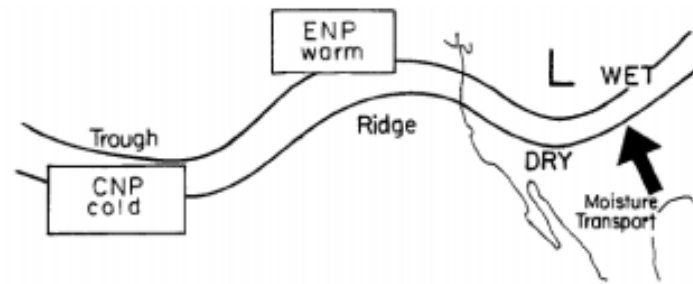
cool phase



monthly values for the PDO index: 1900-September 2009

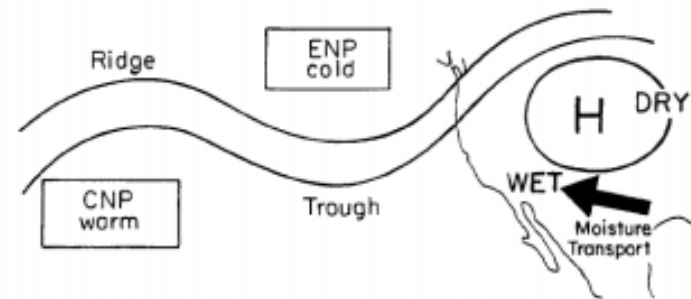


Schematic of relationship between PDO, ENSO and early monsoon period (position of monsoon ridge and mid-level moisture transport)



El Niño

El Niño
High NPO Phase

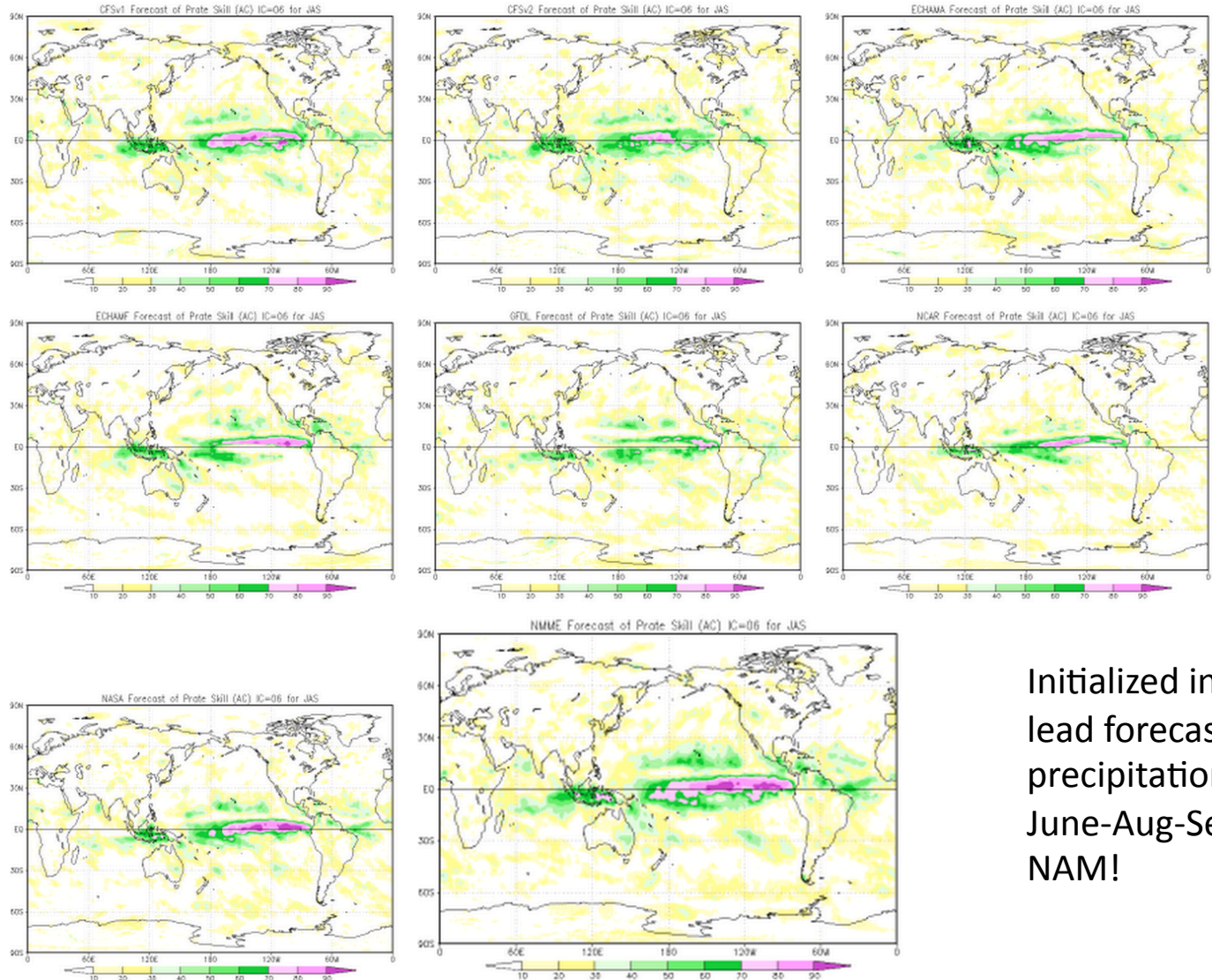


La Niña

La Niña
Low NPO Phase



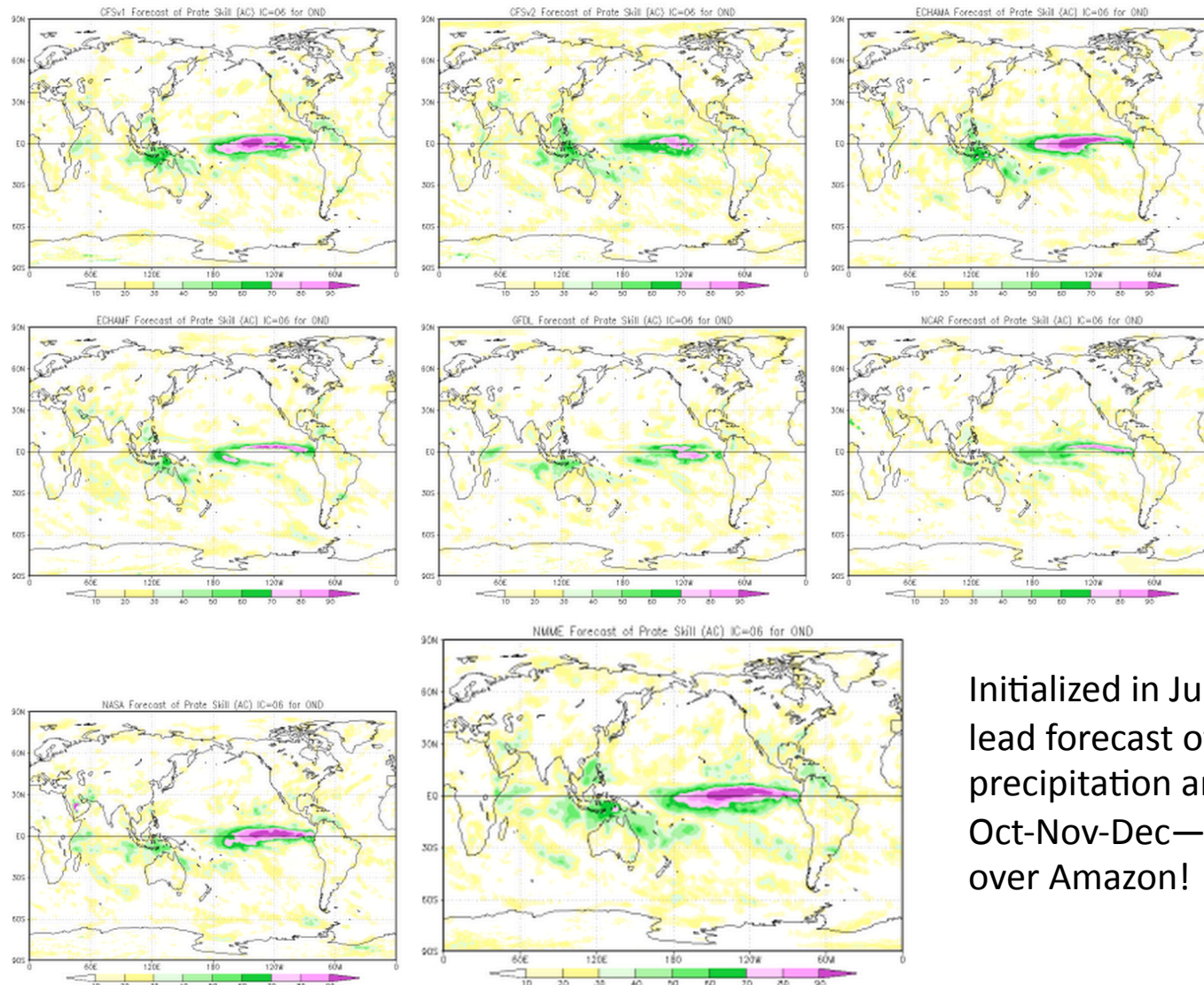
Season 1 prate forecast



Initialized in June. 1 month lead forecast of precipitation anomalies in June-Aug-Sep—No skill over NAM!



Season 4 prate forecast



Initialized in June. 4 month
lead forecast of
precipitation anomalies in
Oct-Nov-Dec—Some skill
over Amazon!

References

- Gutzler, 2000: An index of interannual precipitation variability in the core of the North American Monsoon region. *J. Climate*, 17, 4473-4480.
- Krishnamurthy, V. and V. Misra, 2011: Daily atmospheric variability in the South American Monsoon System. *Clim. Dyn.*, doi.10.1007/s00382-010-0881-4.
- Misra, V., 2009: Coupled Air, Sea, and Land Interactions of the South American Monsoon. *J. Climate*, 21, 6389-6403
- Ropelewski, C., 2005: The North American Monsoon System. WMO Tech. Doc. 1266 (TMPR Rep. 70), 207-218
- Mechoso, C., 2005: The American Monsoon System. WMO Tech. Doc. 1266, (TMPR REP. 70), 196-208.
- Reports to the Nation: The North American Monsoon. Available from http://www.cpc.ncep.noaa.gov/products/outreach/Report-to-the-Nation-Monsoon_aug04.pdf